

Accumulation of Salicylic Acid and 12-oxo-phytodienoic Acid Acting on the Antioxidant Pathway to Keep Stability of Striped Leaves of Variegated Temple Bamboo

Lingyan Chen, Yu Tang, and Yun Tao

College of Landscape Architecture and Art, Fujian Agriculture and Forestry University, No. 15 Shangxiadian Road, Cangshan District, Fuzhou, Fujian 350002, China

Azra Seerat

College of Forestry, Fujian Agriculture and Forestry University, No. 15 Shangxiadian Road, Cangshan District, Fuzhou, Fujian 350002, China

Pengkai Zhu, Tianyou He, and Yushan Zheng

College of Landscape Architecture and Art, Fujian Agriculture and Forestry University, No. 15 Shangxiadian Road, Cangshan District, Fuzhou, Fujian 350002, China

KEYWORDS. 12-oxo-phytodienoic acid, antioxidant capacity, chloroplast, salicylic acid, *Sinobambusa tootsik* f. *luteolalbostrata*

ABSTRACT. Variegated temple bamboo (*Sinobambusa tootsik* f. *luteolalbostrata*) is one of the native variegated bamboo species has some whole green (WG) and whole white (WW) leaves in addition to striped green and white ones. The life span of WW leaves is short, but the life span of striped leaves (SLs) is unaffected by the area of white mesophyll, and the SL phenotype is well maintained. To explore the mechanism of phenotypic stability of SL, we took five leaf phenotypes as study materials: WG, WW, SL, the green part of SL (SG), and the white part of SL (SW). Through the measurement of photosynthetic pigments, leaf nutrient elements, chloroplast synthesis-related hormones and their precursors in the leaves, and antioxidant system parameters, we examined the antioxidant adaptation mechanism of the white mesophyll cells of *S. tootsik* f. *luteolalbostrata*. The results indicated that abscisic acid (ABA) levels were substantially higher in WW leaves than in SW leaves, and salicylic acid (SA) levels were significantly higher in SW leaves compared with WW leaves. Levels of 12-oxo-phytodienoic acid (OPDA), and SA were substantially higher in WW and SW than in the leaves of the other three phenotypes. Glutathione (GSH) levels were substantially higher in SW than in SG and reactive oxygen species (ROS) levels were significantly lower. Overall, the white mesophyll cells of *S. tootsik* f. *luteolalbostrata* had strong antioxidant properties. SA and OPDA jointly act on the antioxidant pathway to reduce the content of ROS in leaves, thus ensuring the stability of SL.

It has been shown by numerous studies on leaf color mutants that mesophyll cells that are yellow or white may survive despite abnormalities in the chloroplasts (Chen 2008; Wang 2016). But how do yellow or white mesophyll cells maintain their ability to grow and develop due to reduced metabolic capacity? Even in terms of temperature regulation, water vapor transport, ultraviolet protection, light protection, and low-temperature adaptation, some leaf color mutants have stronger resistance than green cells (Liu et al. 2001). It remains unknown whether these leaf color-deficient cells can use specific metabolites as signals to “communicate” with the nucleus to maintain their survival.

Chloroplast-deficient variegated plants often exhibit poorly developed chloroplasts and broken thylakoid membrane structures

(Chen et al. 2018). Chloroplasts are not only the center of photosynthesis and responsible for the transformation of plant energy, but also the central organ for the synthesis of important cellular molecules in plants, including amino acids, fatty acids, carbohydrates, vitamins, and phytohormone, such as ABA, SA, and jasmonates, including jasmonic acid (JA) and jasmonoyl-isoleucine (JA-Ile) (Chi et al. 2015). Among the hormones synthesized by plant chloroplasts, acidic phytohormones play an important role in the growth and development of plant cells as well as in biotic and abiotic stress responses (Zhu et al. 2017). Among them, SA, ABA, and jasmonates are associated with plant leaf senescence mechanisms. Chloroplasts can modify adjacent subcellular structures and produce phytohormones, which act as signals to relieve biotic and abiotic stresses on plants, to sustain plant cell survival, and maintain their function (Sakamoto et al. 2002). These signaling substances have the potential to regulate nuclear gene expression through negative signaling pathways (Yu et al. 2007). For example, melon (*Cucumis melo*) treated with OPDA and SA can significantly reduce the systemic transmission of the virus by regulating the increase of pathogen-induced callose deposits through signal transduction (Fernandez-Crespo et al. 2017). ABA prevents the toxic effects of ROS by slowing down the activity of

Received for publication 5 Oct 2023. Accepted for publication 1 Dec 2023.

Published online 23 Jan 2024.

This research was funded by the Scientific Research Project of Fujian Province, grant number 2023J01478.

L.C. and Y. Tang contributed equally to this work.

Y.Z. is the corresponding author. E-mail: zys1960@163.com.

This is an open access article distributed under the CC BY-NC-ND license (<https://creativecommons.org/licenses/by-nc-nd/4.0/>).

enzymes such as superoxide dismutase and catalase (CAT); SA can reduce the accumulation of hydrogen peroxide (H_2O_2), reduce cell damage by free radicals, reduce malondialdehyde (MDA) content, and influence plant response to adversity stress by regulating the plant antioxidant system (Wang and Wang 2012).

In variegated plants, photosynthesis is blocked due to the lack of chlorophyll in the white mesophyll part and the physiological activities associated with it cannot be carried out (Chen et al. 2018). To avoid early senescence of the white mesophyll cells, plants activate leaf ROS scavenging processes through endogenous hormone signaling. In the study of two cultivars of *Epipremnum aureum*, ‘Marble Queen’ (white-spotted colored leaves) and ‘Golden Pothos’ (yellow-spotted colored leaves), it was found that the white mesophyll cells had significantly elevated levels of OPDA and its related complexes were transmitted as signaling molecules to the nuclei of green mesophyll cells in the same leaves, upregulating genes related to resistance and ROS scavenging in white mesophyll cells, resulting in a decrease in ROS content, protecting the survival of white mesophyll cells (Sun et al. 2017), enabling the persistent color leaf phenotype of *Epipremnum aureum*.

Variegated temple bamboo (*S. tootsik* f. *luteoloalbostrata*) is a species of variegated ornamental bamboo native to Fujian Province. It can grow to a height of 3 to 5 m and has three phenotypes: WG, WW, and SL on the same plant, and variegated performance enhances their ornamental value. In cultivation, it was found that its WW leaves are short-lived and usually fall off within 3 weeks, and senesce quickly, whereas the SL does not differ significantly in senescence rate due to the increase or decrease of white mesophyll cell area (Han et al. 2005). A previous study on *S. tootsik* f. *luteoloalbostrata* clarified the existence of chloroplast structural defects in its white mesophyll cells. White mesophyll cells had negligible amounts of damaged plastids or no broken plastid structure at all (Chen et al. 2019b). How do the plants protect white mesophyll cells and maintain the phenotypes? Do the mesophyll cells of different phenotypes have specific hormone regulation mechanisms?

In this study, we used the leaves of different phenotypes of *S. tootsik* f. *luteoloalbostrata* as research materials to explore the role of chloroplast synthesis-related hormones in leaf antioxidant function by measuring photosynthetic pigment, nutrient content, hormone content associated with chloroplast production, and antioxidant capacity in the different phenotypic leaves of *S. tootsik* f. *luteoloalbostrata*. In addition to providing important insights on the maintenance of chloroplast-deficient mesophyll cells, this study can lay a theoretical basis for the breeding of variegated bamboo species.

Materials and Methods

PLANT MATERIAL. Twenty-one 2-year-old *S. tootsik* f. *luteoloalbostrata* were bought from a local nursery on 10 Mar 2016. All plants were planted in seven planting grooves (60 cm wide, 3 m long, and 50 cm deep) with each groove planted for every three plants using a mixture of sand and topsoil (1:1 v/v) and were grown under 30% shade at the Bamboo Research Institute, Fujian Agriculture and Forestry University, Fuzhou, Fujian Province, China (lat. 26°5′N, long. 119°13′E, elevation 12 m), where the average solar radiation per year is $\approx 1246 \text{ kW}\cdot\text{h}\cdot\text{m}^{-2}$. The average air temperature during the growing season (from

March to August) was 27.6°C/19.7°C (day/night), and the relative humidity was between 50% and 65%. The frequency of watering the plants depended on rainfall and temperature, ensuring that plants had a sufficient water supply. Each plant was applied with 0.5 kg base manure with 45% organic material (0.8N–0.3P–0.4K granular biological organic fertilizer; Nengliangdan, Shijiazhuang, Hebei, China) while spraying 200 mL of 5 g·L⁻¹ compound fertilizer (10N–3.5P–5.8K water-soluble compound fertilizer; Nengliangdan, Shijiazhuang, Hebei, China) every 15 d from May to August.

On 15 Apr 2022, the fully developed leaves on the annual branches of *S. tootsik* f. *luteoloalbostrata* (cutting height 1.5 m) were chosen for the experiment when the daily average maximum temperature reached 25°C in the spring of that year. SLs were collected, and part of the SLs were divided into white and green to obtain the white part of SLs (SW) and the green part of SLs (SG). At the same time, WG and WW leaves were collected as the control group (Fig. 1). The quantity of material collected was established based on the needs of each component of the experiment, petioles were removed from all leaves, and the remaining leaves were washed with pure water for use.

DETERMINATION OF PHOTOSYNTHETIC PIGMENT CONTENT IN DIFFERENT LEAF COLOR PHENOTYPES. About 15 to 20 fresh leaves (0.25 g) per phenotypes (SL, SG, SW, WG, WW) were collected as one sample, leaves were cut into 0.1 × 0.1-cm pieces, and three replications were prepared. Then, each sample was immersed in a 25-mL solution of acetone and anhydrous ethanol (1:1, v/v) for 48 h in the dark until all the pieces turned completely white. The chlorophyll content was determined by measuring the optical density (OD) of the liquid extract at 470, 663, and 645 nm using a spectrophotometer (TU-1900; Persee, Pinggu, Beijing, China). For each sample, three readings of OD were recorded, with 36 readings in total. The total content was calculated using the following equations:

$$Chla = (12.72 \times A_{663} - 2.59 \times A_{645}) \times V / (1000 W) \quad [1]$$

$$Chlb = (22.88 \times A_{645} - 4.67 \times A_{663}) \times V / (1000 W) \quad [2]$$

$$Chla + b = (20.29 \times A_{645} + 8.04 \times A_{663}) \times V / (1000 W) \quad [3]$$

$$Cars = (A_{470} \times V / W - 2.05 \times Chla - 114.8 \times Chlb) / 245 \quad [4]$$

where Chla, Chlb, Chla+b, and Cars represent chlorophyll a, chlorophyll b, total chlorophyll content, and carotenoid content ($\text{mg}\cdot\text{g}^{-1}$), respectively, V stands for the total volume of liquid extract (mL), and W stands for the weight of one sample (g).

DETERMINATION OF KEY NUTRIENTS. Twenty to 25 leaves for each phenotype (SL, SG, SW, WG, WW) from annual branches were collected. Following a 48-hour oven-drying process at 75°C to achieve a stable weight, the samples were powdered to fit through a 0.425-mm screen. A sample of $0.5 \pm 0.005 \text{ g}$ of fine-powder oven-dried leaf tissue was weighed, placed into 40-mL crucible tubes, and ashed at 500°C for 16 h. At a temperature of less than 200°C, the furnace door was carefully opened to prevent the ashy leaf samples from being oxidized by the fast air intake. The ashed samples were equilibrated with 15 mL 0.5 M HCl at room temperature for 30 min using an adjustable macro-pipette to digest the ashes. The sample solution was decanted into 25-mL glass tubes and kept at $< 4^\circ\text{C}$ pending analysis. The sample solution was analyzed for phosphorus (P), potassium (K), calcium (Ca), magnesium (Mg), copper (Cu), iron (Fe), manganese (Mn), zinc (Zn), and sodium (Na) by inductively coupled plasma mass spectrometry [ICP-MS (NexION 300X;



Fig. 1. Three phenotypes of leaves of *Sinobambusa tootsik* f. *luteoalbostrata*. *Sinobambusa tootsik* f. *luteoalbostrata* has three phenotypes: whole green (WG), whole white (WW), and striped leaf (SL).

Thermo Fisher Scientific, Waltham, MA, USA)]. An elemental analyzer (EMA 502 CHNS-O; VELP Scientifica, Usmate Velate, Lombardy, Italy) was used to analyze nitrogen (N) (Herrera-Vasquez et al. 2015).

DETECTION OF HORMONE LEVELS ASSOCIATED WITH CHLOROPLAST SYNTHESIS. Leaf hormones (JA, JA-Ile, OPDA, ABA, and SA) from SL, SG, SW, WG, and WW were extracted according to Shi et al. (2009) with some modifications. Three replicate 0.3-g leaf samples (about 20–25 leaves) of five phenotypes (SL, SG, SW, WG, WW) were collected. Leaf tissues of each sample were ground with a mortar and pestle in liquid nitrogen to powder. The sample ($n = 75$) was extracted in 3 mL hexanitrile, and the hormones were extracted for 12 h in a 4 °C refrigerator. The mortars, pestles, and reagents were precooled to 4 °C; all operations were conducted on ice and the extraction process was conducted in the dark. After centrifugation at 12,000 g_n at 4 °C for 5 min, the supernatant was removed and stored, and then 1.5 mL hexanitrile was added to resuspend the precipitate. The solution was held at 4 °C for 4 h and then centrifuged again at the same intensity, and the supernatant was mixed with the previous

supernatant. The combined extraction solution was centrifuged again at the same intensity and the precipitate was discarded. Then 15 mg C18 packing material was added to the supernatant, shaken vigorously for 30 s, centrifuged at 10,000 g_n for 5 min, and the supernatant was taken. The hexonitrile in the supernatant was evaporated under flowing nitrogen, the remaining aqueous phase was frozen at –80 °C, and the sample was then freeze-dried. The residue was dissolved in 200 μ L methanol, passed through a 0.22- μ m filter membrane, and put into a –20 °C refrigerator for testing.

The analysis was performed with a high-performance liquid chromatograph [HPLC (1290 Infinity II; Agilent Technologies, Santa Clara, CA, USA)]. The analytical procedure used a C18 reverse-phase chromatographic column [150 mm \times 2.1 mm, 2.7 μ m (InfinityLab Poroshell 120 SB-C18, Agilent Technologies)] at 30 °C. The analytes were eluted with water (mobile phase A) and methanol (B) in 0.1% formic acid in a gradient: 0–1 min B at 20%, 1–3 min B increasing from 20% to 50%, 3–9 min B increasing to 80%, 9–13 min at 80%, 13–14 min B from 80% to 100%, and 14–17 min B decreasing from 100% to 20%. The injecting volume was 2 μ L and the flow rate was 0.3 mL \cdot min $^{-1}$.

DETECTION OF GLUTATHIONE (GSH) AND ROS CONTENT. Three 0.1-g replicate leaf samples (~10–15 leaves) of five phenotypes (SL, SG, SW, WG, WW) were used. The concentrations of GSH, oxidized glutathione (GSSG), and total glutathione were determined by using the GSH assay kit (GSH-1-W; Keming, Suzhou, Jiangsu, China) and GSSG assay kit (GSSG-1-W, Keming) in accordance with the manufacturer's instructions as described. The GSH/GSSG ratio was calculated based on GSH and GSSG concentration. Moreover, the measurements of H_2O_2 and superoxide anion (O_2^-) concentrations were, respectively, performed by using H_2O_2 assay kit (H_2O_2 -1-Y, Keming) and O_2^- assay kit (SA-1-G, Keming).

STATISTICAL ANALYSIS. All the data were analyzed using statistical software (IBM SPSS Statistics version 19.0; IBM Corp., Armonk, NY, USA). A one-way analysis of variance and the statistical significance ($P < 0.05$) of mean variations between different treatments was determined using Tukey's honestly significant difference test. All the values are presented as mean with \pm as the standard error. The spreadsheet software (Microsoft Excel 2016; Microsoft Corp., Redmond, WA, USA) was used for visualization and tables. Means and standard errors were calculated from three replicates.

Results

DETERMINATION OF PHOTOSYNTHETIC PIGMENT CONTENT OF DIFFERENT LEAF PHENOTYPES. The overall photosynthetic pigment content of the leaves of *S. tootsik* f. *luteolalbostrata* showed significant differences in WG and SG $>$ SL $>$ WW and SW. In WG and SG leaves, the contents of chlorophyll a (Chla), chlorophyll b (Chlb), and carotenoids (Cars) were not significantly different, that is, there was no significant difference in the distribution of photosynthetic pigments in the green part leaves. In WW and SW, the contents of Chla, Chlb, and Cars were also not significantly different, that is, there was no significant difference in the distribution of photosynthetic pigments in the white part leaves. Compared with WG, the chlorophyll (a+b) (Chla+b) content of WW and the SW accounted for 0.75% and 0.80% of WG, respectively, and the carotenoid content was 6.13% and 6.86% of WG. It shows that the difference in chlorophyll content is the main reason for the difference in the leaf color of *S. tootsik* f. *luteolalbostrata* (Table 1).

ANALYSIS OF NUTRIENT ELEMENTS IN DIFFERENT PHENOTYPES OF LEAVES. Among a large number of elements, the contents of N, P, K, and Mg were not significantly different among the five leaf types of *S. tootsik* f. *luteolalbostrata*, and the content of Ca element closely related to signal transduction in SL was significantly higher than that in WW and WG (Fig. 2).

In terms of trace elements, the contents of Mn and Cu elements in leaves of five types were not significant. Compared with the other four leaf kinds, the content of Na in WW was noticeably less at $69.03 \text{ mg}\cdot\text{kg}^{-1}$. Compared with the other three leaf types, SW and WW have substantially less Fe than the other three (Fig. 3).

DIFFERENCES IN HORMONE LEVELS ASSOCIATED WITH CHLOROPLAST SYNTHESIS. The contents of SA, ABA, OPDA, JA, and JA-Ile were determined in different phenotypes of leaves of *S. tootsik* f. *luteolalbostrata*, and the results were as follows: The content of SA of the five leaf phenotypes generally showed a significant difference, with $22,509.71 \text{ ng}\cdot\text{g}^{-1}$ in SL $>$ $14625.67 \text{ ng}\cdot\text{g}^{-1}$ in WG $>$ $9903.11 \text{ ng}\cdot\text{g}^{-1}$ in WW (Fig. 4A). In contrast, the SA content of the SW was 1.92 times higher than the WW, and this difference was substantial.

The content of ABA of the five leaf phenotypes showed significant differences, with the overall performance of $15.45 \text{ ng}\cdot\text{g}^{-1}$ in WG $>$ $13.56 \text{ ng}\cdot\text{g}^{-1}$ in WW $>$ $5.52 \text{ ng}\cdot\text{g}^{-1}$ in SL; among them, the SG was $12.20 \text{ ng}\cdot\text{g}^{-1}$ $>$ the SW was $2.68 \text{ ng}\cdot\text{g}^{-1}$. Comparing the WW and SW, it was found that the content of ABA in WW was significantly higher than in SW, which was 5.06 times higher (Fig. 4B).

OPDA is a precursor of JA synthesis, which can increase the resistance of mesophyll cells and increase the excretion of oxygen free radicals to protect cells. The content of OPDA of the five leaf phenotypes showed significant differences, with the overall performance of $45.25 \text{ ng}\cdot\text{g}^{-1}$ in WW $>$ $28.01 \text{ ng}\cdot\text{g}^{-1}$ in SL $>$ $23.15 \text{ ng}\cdot\text{g}^{-1}$ in WG; the SW ($44.08 \text{ ng}\cdot\text{g}^{-1}$) was significantly higher than the SG ($28.08 \text{ ng}\cdot\text{g}^{-1}$), that is, the content of OPDA in SW was 1.57 times that of SG. It shows that the content of OPDA in white mesophyll cells in the leaves of *S. tootsik* f. *luteolalbostrata* was significantly higher than that in green mesophyll cells, and the content of OPDA in different phenotypes of green mesophyll cells is not significantly different, and the content of OPDA in different types of white mesophyll cells is not significantly different (Fig. 4C).

OPDA is converted into JA after a series of reduction enzyme reactions. On detection, the content of JA of five leaf phenotypes varied significantly, with the overall performance of WG ($342.03 \text{ ng}\cdot\text{g}^{-1}$) $>$ SL ($260.21 \text{ ng}\cdot\text{g}^{-1}$) $>$ WW ($214.99 \text{ ng}\cdot\text{g}^{-1}$): SG ($642.41 \text{ ng}\cdot\text{g}^{-1}$) $>$ SW ($522.45 \text{ ng}\cdot\text{g}^{-1}$) (Fig. 4C). Compared with the white mesophyll part, the conversion amount of WW during the conversion of OPDA to JA was significantly lower than that of SW, with the content of JA in WW only being 41.15% of SW.

JA-Ile is a product formed by the combination of JA and isoleucine, and its content is correlated with the content of JA. The experimental results showed that the content of JA-Ile of the five leaf phenotypes was consistent with the variation trend of the content

Table 1. Content of photosynthetic pigments in leaves of different phenotypes of *Sinobambusa tootsik* f. *luteolalbostrata*.

Phenotypes	Chla/(mg·g ⁻¹)	Chlb/(mg·g ⁻¹)	Chl(a+b)/(mg·g ⁻¹)	Cars/(mg·g ⁻¹)
Striped leaf (SL)	0.942 ± 0.074 b (52.77)	0.165 ± 0.034 b (47.55)	1.107 ± 0.041 b (51.95)	0.235 ± 0.023 b (57.60)
The green part of SL (SG)	1.784 ± 0.090 a (99.94)	0.316 ± 0.030 a (91.35)	2.100 ± 0.061 a (98.55)	0.431 ± 0.033 a (105.64)
The white part of SL (SW)	0.011 ± 0.000 c (0.62)	0.006 ± 0.001 c (1.73)	0.017 ± 0.001 c (0.80)	0.028 ± 0.001 c (6.86)
Whole green (WG)	1.785 ± 0.006 a (100)	0.347 ± 0.012 a (100)	2.131 ± 0.014 a (100)	0.408 ± 0.011 a (100)
Whole white (WW)	0.012 ± 0.000 c (0.67)	0.005 ± 0.001 c (1.44)	0.016 ± 0.001 c (0.75)	0.025 ± 0.004 c (6.13)

Note: Chla, Chlb, Chla+b, and Cars represent chlorophyll a, chlorophyll b, total chlorophyll content, and carotenoid content (mg·g⁻¹), respectively. Different lowercase letters after the same column of numbers indicate significant differences between different treatments ($P < 0.05$). The value in parentheses is the ratio of that value to the control group (%). The control group was WG.

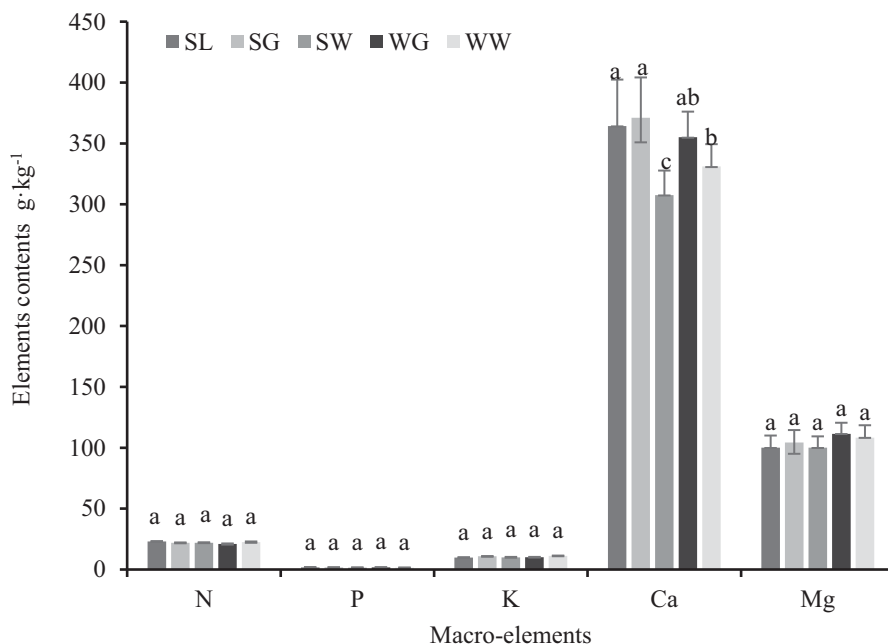


Fig. 2. Differences in macronutrient contents of different leaf phenotypes of *Sinobambusa tootsik* f. *luteoalbostrata*. SL, SG, SW, WG, and WW refer to the striped leaf, the green part of the striped leaf, the white part of the striped leaf, whole green, and whole white, respectively. Duncan grouping was made within each precursor [mean \pm SE (n = 3)]. Where the same lowercase letter appears above the vertical bar, values do not differ significantly at $P < 0.05$.

of JA, with the overall performance of WG ($383.60 \text{ ng}\cdot\text{g}^{-1}$) > SL ($314.42 \text{ ng}\cdot\text{g}^{-1}$) > WW ($253.61 \text{ ng}\cdot\text{g}^{-1}$): SG > SW (Fig. 4C).

DIFFERENCES IN GSH CONTENT OF LEAVES OF DIFFERENT PHENOTYPES. GSH is an important substance for plants to resist oxidative stress and prevent aging. GSH exists in two forms: GSH and GSSG. Among them, GSH is the main active substance and has the effect of eliminating oxygen free radicals. The total GSH content of the five leaf color phenotypes of *S. tootsik* f. *luteoalbostrata* has

significant differences (as shown in Fig. 5), with the overall performance of WG ($466.95 \text{ nmol}\cdot\text{g}^{-1}$) > WW ($280.88 \text{ nmol}\cdot\text{g}^{-1}$) > SL ($256.24 \text{ nmol}\cdot\text{g}^{-1}$); among which the SW ($352.01 \text{ nmol}\cdot\text{g}^{-1}$) > SG ($166.37 \text{ nmol}\cdot\text{g}^{-1}$). The content of GSH of WG was significantly higher than the other four leaf phenotypes, which was 1.66 times that of WW. The content of GSH in WG was significantly higher than the other phenotypes, and there was no significant difference between WW and SL. However, the content of GSH in SW was

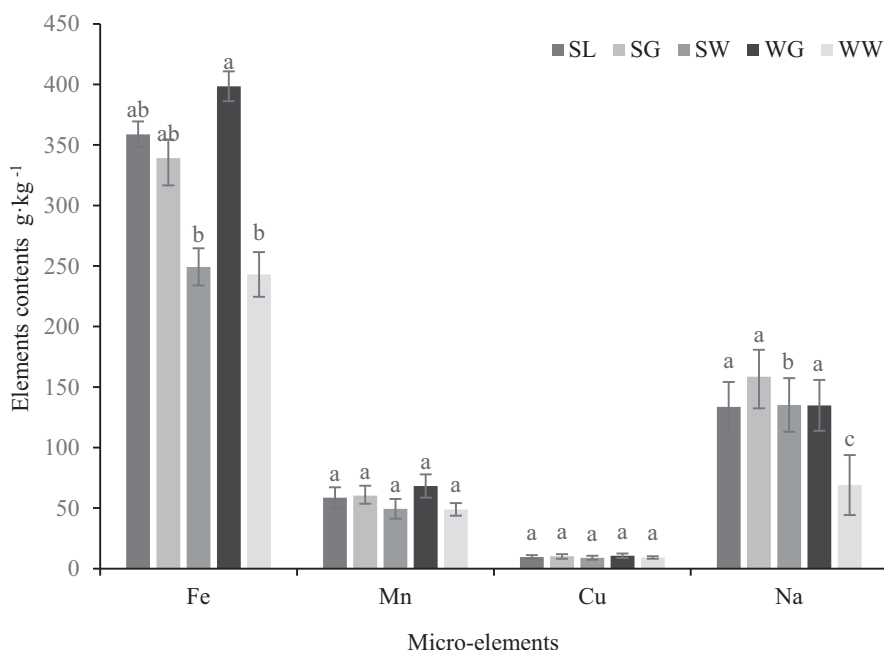


Fig. 3. Differences in micronutrient contents of different leaf phenotypes of *Sinobambusa tootsik* f. *luteoalbostrata*. SL, SG, SW, WG, and WW refer to the striped leaf, the green part of the striped leaf, the white part of the striped leaf, whole green, and whole white, respectively. Duncan grouping was made within each precursor [mean \pm SE (n = 3)]. Where the same lowercase letter appears above the vertical bar, values do not differ significantly at $P < 0.05$.

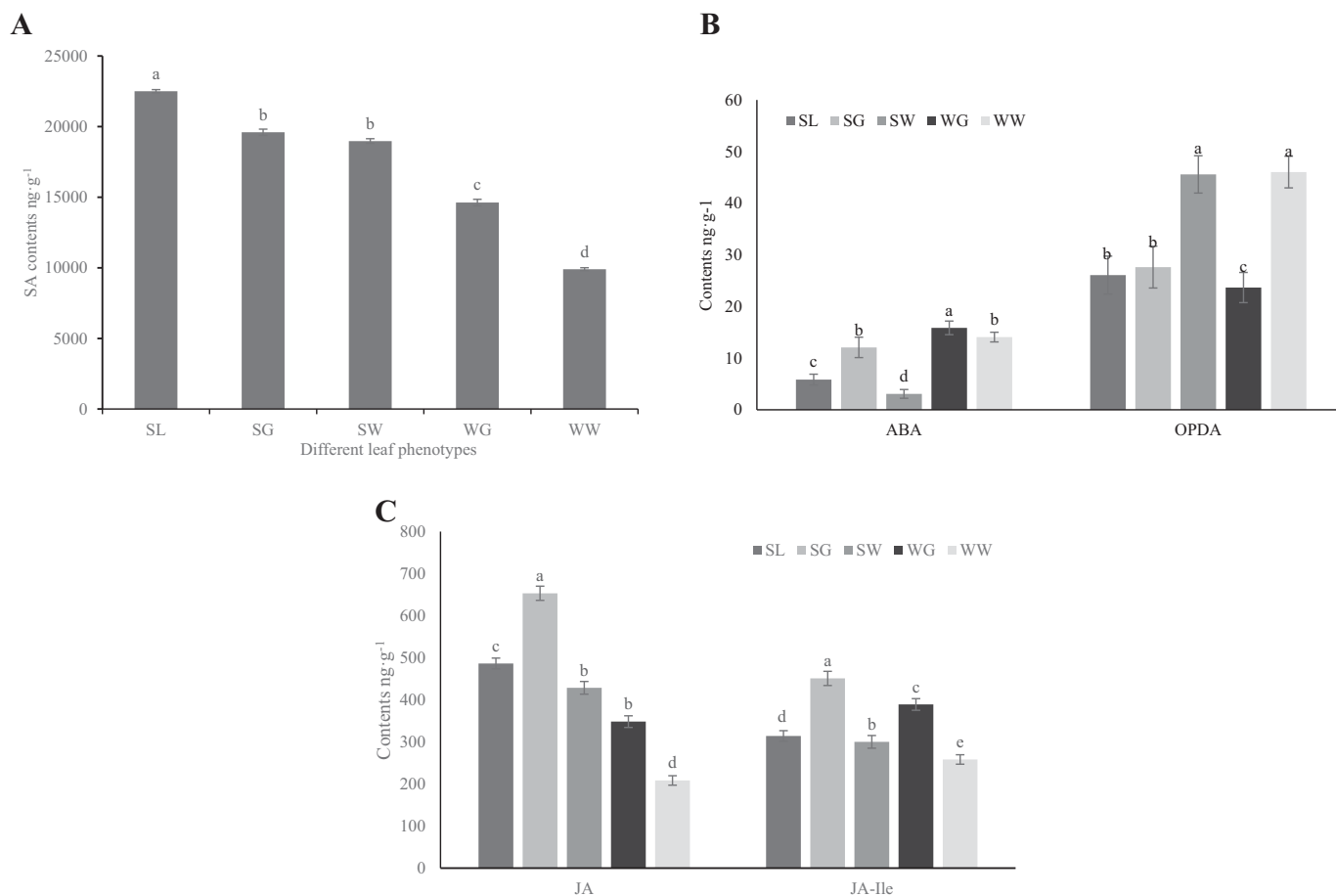


Fig. 4. Phenotypic hormone and hormone precursor content differences in different leaves of *Sinobambusa tootsik* f. *luteoalbostrata*. (A) Salicylic acid (SA) content (ng·g⁻¹) in the leaf phenotypes of five species of *Sinobambusa tootsik* f. *luteoalbostrata*. (B) Absciscic acid (ABA) and 12-oxo-phytodienoic acid (OPDA) contents (ng·g⁻¹) in the leaf phenotypes of five species of *Sinobambusa tootsik* f. *luteoalbostrata*. (C) Jasmonic acid (JA) and jasmonoyl-isoleucine (JA-Ile) contents (ng·g⁻¹) in the leaf phenotypes of five species of *Sinobambusa tootsik* f. *luteoalbostrata*. Note: SL, SG, SW, WG, and WW refer to the striped leaf, the green part of the striped leaf, the white part of the striped leaf, whole green, and whole white, respectively. Duncan grouping was made within each precursor [mean ± SE (n = 3)], where the same lowercase letter appears above the vertical bar, values do not differ significantly at $P < 0.05$.

significantly higher than that in WW. The content of GSSG was generally low (Fig. 5).

DIFFERENCES IN ROS IN LEAVES OF DIFFERENT PHENOTYPES. ROS include highly reactive active substances such as hydroxyl radicals (-OH), O_2^- , and H_2O_2 , among which O_2^- and H_2O_2 are the initial sources of ROS. Excessive ROS in plant cells can lead to lipid peroxidation of plant cell membranes, generating a series of compounds including MDA, which ultimately leads to cell death. Therefore, by measuring the levels of O_2^- and H_2O_2 in different phenotypic leaf tissues of *S. tootsik* f. *luteoalbostrata*, the degree of oxidative stress and differences in antioxidant capacity between different phenotypic leaves can be compared. Many studies showed that the content of O_2^- in the three leaf types varies significantly, with the overall performance of SL ($177.29 \text{ nmol}\cdot\text{g}^{-1}$) > WG ($144.57 \text{ nmol}\cdot\text{g}^{-1}$) > WW ($126.05 \text{ nmol}\cdot\text{g}^{-1}$). However, the differences between the SL and WG were not significant. The SG ($154.91 \text{ nmol}\cdot\text{g}^{-1}$) was significantly higher than the SW ($70.30 \text{ nmol}\cdot\text{g}^{-1}$) (Fig. 6).

The content of H_2O_2 of different leaf phenotypes of *S. tootsik* f. *luteoalbostrata* showed that WG ($18.08 \text{ nmol}\cdot\text{g}^{-1}\cdot\text{mL}^{-1}$) > SL ($11.42 \text{ nmol}\cdot\text{g}^{-1}\cdot\text{mL}^{-1}$) > WW ($5.57 \text{ nmol}\cdot\text{g}^{-1}\cdot\text{mL}^{-1}$), and the SG

($17.67 \text{ nmol}\cdot\text{g}^{-1}\cdot\text{mL}^{-1}$) was significantly higher than the SW ($5.50 \text{ nmol}\cdot\text{g}^{-1}\cdot\text{mL}^{-1}$), which was 3.21 times higher than the SW (Fig. 7).

Discussion

LOW CONTENT OF PHOTOSYNTHETIC PIGMENTS IN WHITE MESOPHYLL CELLS. The photosynthetic pigment content of the three leaf color phenotypes (WG, WW, SL) of *S. tootsik* f. *luteoalbostrata* revealed a general growing tendency as the area of green mesophyll cells increased. In the SL, the SW was similar to the WW, while the SG was similar to the WG that was similar to the research results of *Bambusa multiplex* cv. Silverstripe (Lai et al. 2018).

The main synthesis site of plant photosynthetic pigments is in chloroplasts, which are important light harvesting complexes (Sun et al. 2017). According to the cell ultrastructure of different phenotypes of *S. tootsik* f. *luteoalbostrata* leaves in previous studies, white mesophyll cells had poor or missing chloroplast development, broken or distorted thylakoid membrane structure, and significant differences in white mesophyll cell structures between WW and SL. The chloroplast structure in green mesophyll

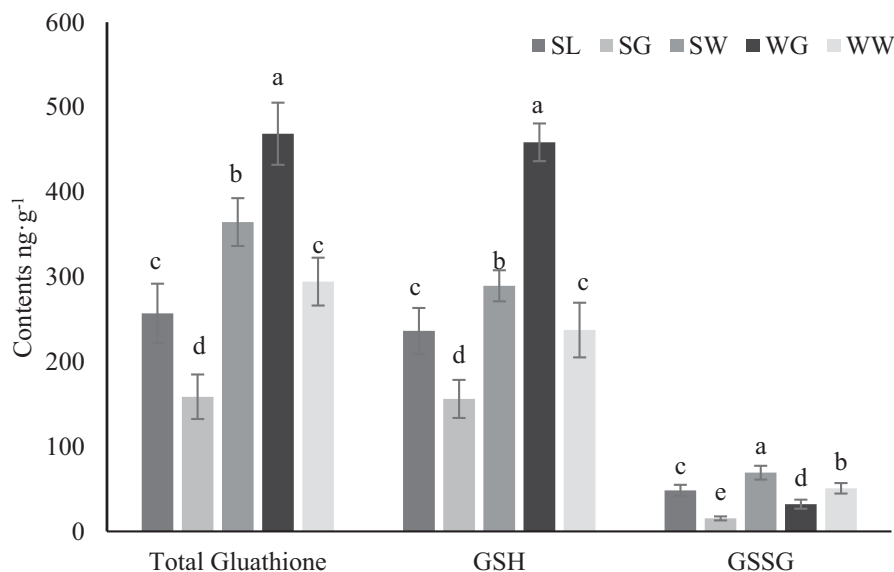


Fig. 5. Differences in glutathione (GSH) content of different leaf phenotypes of *Sinobambusa tootsik* f. *luteoloalbostrata*. SL, SG, SW, WG, and WW refer to the striped leaf, the green part of the striped leaf, the white part of the striped leaf, whole green, and whole white, respectively. Duncan grouping was made within each precursor [mean \pm SE (n = 3)]. Where the same lowercase letter appears above the vertical bar, values do not differ significantly at $P < 0.05$. GSH = glutathione, GSSG = oxidized glutathione.

cells is intact, and there is no obvious difference between green mesophyll cells in WG and SL (Chen et al. 2018). These studies further confirm that cells with chloroplast defects have hindered the synthesis of photosynthetic pigments and low chlorophyll content.

THERE IS NO NUTRIENT DEFICIENCY IN THE WHITE MESOPHYLL CELLS. Plants that are deficient in certain nutrients may experience leaf senescence, yellowing, and slow growth (Jin et al. 2010). To rule out that the color leaf phenomenon of *S. tootsik* f. *luteoloalbostrata* is caused by differences in nutrient elements, this study detected the nutrient content in the leaves of different phenotypes. By comparing the content of 10 major elements in

different leaf color phenotypes of *S. tootsik* f. *luteoloalbostrata*, it was found that there was no significant difference in most nutrient elements among the five leaf types of *S. tootsik* f. *luteoloalbostrata*. Although white mesophyll cells lacked the element of Fe that is directly linked to chlorophyll production, chloroplasts contain more than 90% of the element of Fe found in plants (Wu et al. 2018). However, the experimental materials in this study were all cultivated under the same fertilization conditions. The production of white mesophyll cells in *S. tootsik* f. *luteoloalbostrata* may be related to the reduction in Fe absorption, transport, or efficiency caused by chloroplast structural defects in the leaves, which is similar to the performance of yellow leaf mutants

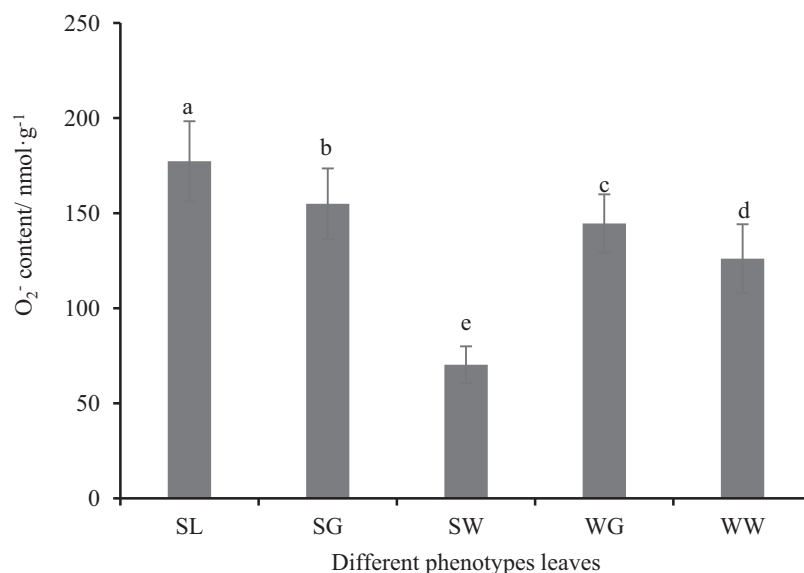


Fig. 6. Differences in superoxide anion (O_2^-) content of different leaf phenotypes of *Sinobambusa tootsik* f. *luteoloalbostrata*. SL, SG, SW, WG, and WW refer to the striped leaf, the green part of the striped leaf, the white part of the striped leaf, whole green, and whole white, respectively. Duncan grouping was made within each precursor [mean \pm SE (n = 3)]. Where the same lowercase letter appears above the vertical bar, values do not differ significantly at $P < 0.05$.

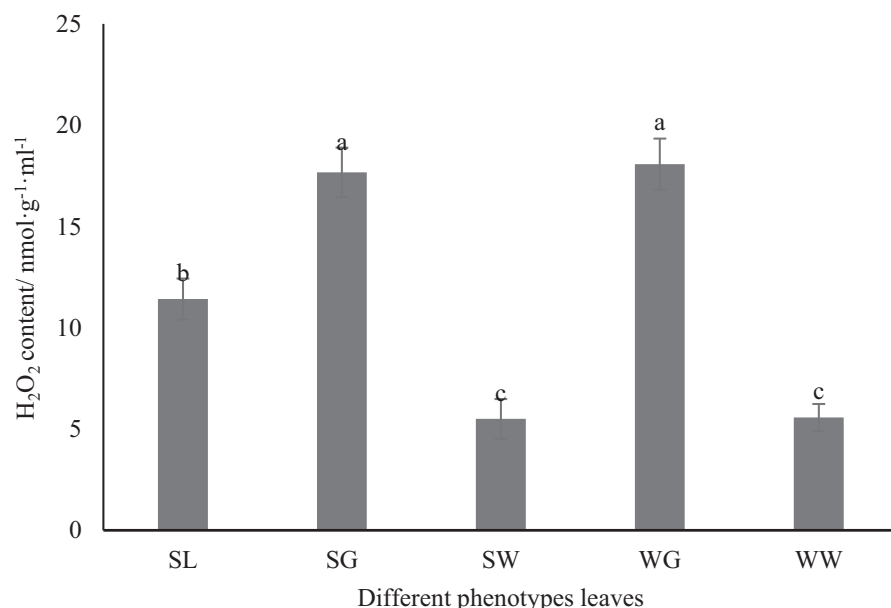


Fig. 7. Differences in the hydrogen peroxide (H₂O₂) content of different leaf phenotypes of *Sinobambusa tootsik* f. *luteoloalbostrata*. SL, SG, SW, WG, and WW refer to the striped leaf, the green part of the striped leaf, the white part of the striped leaf, whole green, and whole white, respectively. Duncan grouping was made within each precursor [mean \pm SE (n = 3)]. Where the same lowercase letter appears above the vertical bar, values do not differ significantly at $P < 0.05$.

in *Brassica napus* after applying Fe nutrient solution (Yin et al. 2016).

Among the three leaf phenotypes of *S. tootsik* f. *luteoloalbostrata*, including WW, WG, and SL, the content of the Ca element of SL was significantly higher than that of the other phenotypes. Ca element is the second messenger of plants and plays a significant role in regulating plant growth and development. Calcium ion (Ca²⁺) can enhance plant resistance, manifested by regulating plant chlorophyll content, stomatal conductance, net photosynthetic rate, etc. to regulate photosynthesis and increase soluble sugar content to achieve antioxidant capacity of cell resistance (Chen et al. 2019a). The Ca content increase in SL indicates their superiority in cellular information transmission.

Overall, there is no nutrient deficiency problem among the leaves of different phenotypes of *S. tootsik* f. *luteoloalbostrata* due to insufficient external nutrient supply. The growth of its white mesophyll cells is mainly regulated by genes.

SA WAS SIGNIFICANTLY ENRICHED IN SLs. In this study, it was found that the content of SA in SL of *S. tootsik* f. *luteoloalbostrata* was significantly enriched, and the content of SA in SW was 1.92 times that of WW. SA is a phenolic hormone that regulates plant growth and development in response to stress, and it also has a positive regulatory function on plant leaf antiaging (Taiz et al. 2023). Many studies have shown that there is a signaling function between SA and ROS (Cheng et al. 2021; Herrera-Vasquez et al. 2015). SA not only promotes oxidation, but also synergistically exerts antioxidant effects with GSH (Han et al. 2013; Herrera-Vasquez et al. 2015). Plants enriched with SA exhibit an increase in the level of GSH and a decrease in GSH/GSSG ratio, while in GSH synthesis deficient mutants, there is a decrease in the transcription levels of SA and *ICS1* genes (Graham et al. 2015; Yang et al. 2018). However, the mechanism by which SA regulates GSH is unclear. A vital synthesis pathway of SA is the isochorismate synthase pathway, in which the precursor of SA, isochorismate (IC) (Huang et al. 2021; Torrens-Spence et al. 2019;

Ullah et al. 2023; Wu et al. 2023), is produced. The synthesis site of IC is the chloroplast (Dempsey et al. 2011), and the SG provides a site for the synthesis and transportation of this precursor, ensuring that SA can act on white mesophyll cells in the same leaf blade. However, WW could not synthesize sufficient SA due to chloroplast deficiency. This is also the reason why the SL traits of *S. tootsik* f. *luteoloalbostrata* can be stably maintained.

OPDA IS HIGHER IN WHITE MESOPHYLL CELLS. OPDA is an important intermediate in the JA-mediated pathway. The connection between OPDA and plant antiaging is mainly reflected in its regulation of the level of ROS. Among the various plant hormones and their precursors synthesized by the chloroplast, OPDA binds to cyclophilin (CYP20-3) to form the cysteine synthase complex, and binds to serine acetyltransferase to form cysteine (Jimenez et al. 2022). The increasing cysteine is metabolized to GSH to alter the redox reaction in cells and change the redox signaling for regulating the expression of OPDA-responsive genes (Laloi and Havaux 2015). Some studies have shown that OPDA can upregulate the synthesis of GSH by activating the dehydroascorbate reductase, glutathione S-transferase (GST), and γ -glutamyl cysteinyl synthase (γ -ECS) (Maynard et al. 2018; Wasternack and Hause 2018), which is an important pathway to clear ROS, resist oxidative stress, and prevent aging (Knieper et al. 2023). In the study of *Melon necrotic spot virus*, OPDA was also confirmed as a candidate factor with a positive regulatory effect on reducing the level of ROS through ROS scavenging (Fernandez-Crespo et al. 2017). In the studies of two cultivars of *Epipremnum aureum* Marble Queen (white-spotted chromatic leaves) and Golden Potho (yellow-spotted chromatic leaves), it was found that the contents of SA and ABA in green mesophyll cells were significantly higher than those in white mesophyll cells, while JA and JA-Ile were not detected. The significantly increased levels of OPDA and its related complexes in white leaf mesophyll cells were transmitted as signaling molecules to the nucleus of green mesophyll cells in the

same leaves, which upregulated genes related to resistance and the excretion of oxygen free radicals, resulting in a decrease in the content of ROS and thus protecting the survival of white mesophyll cells (Sun et al. 2017).

Based on previous research results and combined with the findings of this study, the content of OPDA in white mesophyll cells of *S. tootsik* f. *luteolalbostrata* leaves was significantly higher than that in green mesophyll cells, indicating that OPDA plays a key antioxidant role in white mesophyll cells. Combined with the distribution of JA in the leaves of *S. tootsik* f. *luteolalbostrata*, it can be concluded that the conversion rate of OPDA in white mesophyll cells is low, and OPDA mainly acts on the synthesis of GSH, which has a positive effect on the scavenging of ROS in white mesophyll cells.

LOW LEVELS OF ROS IN THE WHITE MESOPHYLL CELLS. GSH is an antioxidant that is ubiquitous in plant and animal cells. GSH and GSSG constitute total GSH, which can prevent damage caused by ROS such as O_2^- and H_2O_2 in cells. The ratio of GSH to GSSG in plant cells can measure the level of cellular peroxidation. O_2^- and H_2O_2 are the initial sources of ROS, and O_2^- can directly poison cells as an oxidizing substance, or it can be converted into other ROS, such as H_2O_2 and $-OH$; H_2O_2 has strong cytotoxicity and can cause membrane lipid peroxidation, which can diffuse across the membrane.

By studying the differences in the contents of GSH and ROS between different leaf color phenotypes in *S. tootsik* f. *luteolalbostrata*, it was found that the content of GSH in the SW was significantly higher than that in the SG, whereas the contents of O_2^- and H_2O_2 in SW were significantly lower than those in SG. This indicates that the white mesophyll cells have a stronger ability to scavenge ROS, which is consistent with the research of Park et al. (2013). Previous research found that the albino part of the plant can synthesize most of the antioxidant substances (Grant and Loake 2000; Neill et al. 2002). Deng (2009) found that the content of GSH in the albino tissues of the green-white Hibotan-Nishiki cactus (variegated mutant cactus) was significantly higher than that of the near green epidermis by analyzing the ROS metabolism. Yu (2018) found that the antioxidant capacity of the white tissue cells in *Ananas comosus* var. *bracteatus* leaves was higher than that of the green tissue, which is consistent with the results of this study.

Conclusions

OPDA plays an important role in antioxidant pathway in white mesophyll cells. High levels of OPDA ensure the synthesis of GSH in white mesophyll cells, eliminating intracellular oxygen radicals and maintaining the survival of white mesophyll cells. However, the life span of WW is significantly shorter than that of SL. This study found that the content of SA in SW was significantly higher than that of WW, indicating that SA and OPDA act together in the antioxidant pathway to maintain the stability of striped leaf traits by reducing the content of ROS in leaves, thereby ensuring the stability of SLs. In a study of lead stress in *Zygophyllum fabago*, it was found that plants treated with SA had enrichment of OPDA and ABA in their roots and leaves, which may be due to SA regulation of peroxidase to induce the synthesis of two antioxidant hormones (Wu et al. 2013). This provide ideas for OPDA as an intermediate signal for SA regulating GSH. This study lays a preliminary research foundation for analyzing the phenotypic stability of chlorophyll-

deficient variegated plants in terms of hormone regulation. Further studies can be conducted to address the common mechanism of SA and OPDA in the antioxidant pathway of SW.

References Cited

- Chen D, Tang Y, Shi W, Zhang X, Tao J, Zhao D. 2019a. Progress in the regulation of calcium growth and development. *Mol Plant Breed*. 17(11):3593–3601. <https://doi.org/10.13271/j.mpb.017.003593>.
- Chen L, Lai J, He T, Rong J, Tarin MWK, Zheng Y. 2018. Differences in photosynthesis of variegated temple bamboo leaves with various levels of variegation are related to chlorophyll biosynthesis and chloroplast development. *J Am Soc Hortic Sci*. 143(2):144–153. <https://doi.org/10.21273/JASHS04359-18>.
- Chen L, Xie D, Rong J, Lai J, Lin X, Zheng Y. 2019b. Effects of photosynthetic pigment content on photosynthetic characteristics of different leaf color phenotypes of *Sinobambusa tootsik* f. *luteolalbostrata*. *Linze Kexue*. 55(12):21–31. <https://doi.org/10.11707/j.1001-7488.20191203>.
- Chen Y. 2008. Study on growth rhythm and cutting propagation technology of ornamental bamboo (MS Thesis). Fujian Agriculture and Forestry University, Fuzhou, Fujian, China. <https://doi.org/10.7666/d.y1450331>.
- Cheng F, Gao M, Lu J, Huang Y, Bie Z. 2021. Spatial-temporal response of reactive oxygen species and salicylic acid suggest their interaction in pumpkin rootstock-induced chilling tolerance in watermelon plants. *Antioxidants*. 10(12):2024. <https://doi.org/10.3390/antiox10122024>.
- Chi W, Feng P, Ma J, Zhang L. 2015. Metabolites and chloroplast retrograde signaling. *Curr Opin Plant Biol*. 25:32–38. <https://doi.org/10.1016/j.pbi.2015.04.006>.
- Dempsey DA, Vlot AC, Wildermuth MC, Klessig DF. 2011. Salicylic acid biosynthesis and metabolism. *Arabidopsis Book*. 9:E0156. <https://doi.org/10.1199/tab.0156>.
- Deng B. 2009. Albino plant and higher endogenous reactive oxygen species toxicity (MS Thesis). Lanzhou University, Lanzhou, Gansu, China. <https://doi.org/10.7666/d.Y1516858>.
- Fernandez-Crespo E, Navarro JA, Serra-Soriano M, Finiti I, Garcia-Agustin P, Pallas V, Gonzalez-Bosch C. 2017. Hexanoic acid treatment prevents systemic MNSV movement in *Cucumis melo* plants by priming callose deposition correlating SA and OPDA accumulation. *Front Plant Sci*. 8:1793. <https://doi.org/10.3389/fpls.2017.01793>.
- Graham N, Caroline L, Amna M. 2015. The metabolomics of oxidative stress. *Phytochemistry*. 112:33–53. <https://doi.org/10.1016/j.phytochem.2014.09.002>.
- Grant JJ, Loake GJ. 2000. Role of reactive oxygen intermediates and cognate redox signaling in disease resistance. *Plant Physiol*. 124(1): 21–29. <https://doi.org/10.1104/pp.124.1.21>.
- Han C, He Q, Li Y, Wu H. 2005. A study on effects of paclobutrazol on the growth of ornamental bamboos. *J Bamboo Res*. 24(2):23–25. <https://doi.org/10.3969/j.issn.1000-6567.2005.02.006>.
- Han Y, Chaouch S, Mhamdi A, Queval G, Zechmann B, Noctor G. 2013. Functional analysis of Arabidopsis mutants points to novel roles for glutathione in coupling H_2O_2 to activation of salicylic acid accumulation and signaling. *Antioxid Redox Signal*. 18(16):2106–2121. <https://doi.org/10.1089/ars.2012.5052>.
- Herrera-Vasquez A, Salinas P, Holuigue L. 2015. Salicylic acid and reactive oxygen species interplay in the transcriptional control of defense genes expression. *Front Plant Sci*. 6:171. <https://doi.org/10.3389/fpls.2015.00171>.
- Huang H, Zhan Q, Qin L, Peng Z, Xia S. 2021. Advances in salicylic acid biosynthetic pathways and its regulation in plants. *Acta Laser Biol Sin*. 30(1):22–29. <https://doi.org/10.3969/j.issn.1007-7146.2021.01.003>.
- Jimenez AG, Thirumalaikumar VP, Jander G, Fernie AR, Skirycz A. 2022. OPDA, more than just a jasmonate precursor. *Phytochemistry*. 204:113432. <https://doi.org/10.1016/j.phytochem.2022.113432>.

- Jin M, Wang W, Yu Y. 2010. Differences between several common crop nutrient disorders and similar diseases. *Mod Agric Sci Technol*. 39(24):185–187. <https://doi.org/10.3969/j.issn.1007-5739.2010.24.119>.
- Knieper M, Viehhauser A, Dietz KJ. 2023. Oxylinins and reactive carbonyls as regulators of the plant redox and reactive oxygen species network under stress. *Antioxidants*. 12(4):814. <https://doi.org/10.3390/antiox12040814>.
- Lai J, Li X, Chen L, Rong J, Zheng Y. 2018. Photosynthetic characteristics of three different colors of leaves of *Bambusa multiplex* cv. *Silverstrip*. *Shengtai Huanjing Xuebao*. 27(2):255–261. <https://doi.org/10.16258/j.cnki.1674-5906.2018.02.008>.
- Laloi C, Havaux M. 2015. Key players of singlet oxygen-induced cell death in plants. *Front Plant Sci*. 6:39. <https://doi.org/10.3389/fpls.2015.00039>.
- Liu J, Xu J, Ye S, Chen Z, Huang G. 2001. Study on the regulation of paclobutrazol on the growth of purple bamboo. *J Eng (Stevenage)*. 15(S1):58–59. <https://doi.org/10.3969/j.issn.1000-8101.2001.z1.032>.
- Maynard D, Gröger H, Dierks T, Dietz K-J. 2018. The function of the oxylipin 12-oxophytodienoic acid in cell signaling, stress acclimation, and development. *J Expt Bot*. 69(22):5341–5354. <https://doi.org/10.1093/jxb/ery316>.
- Neill S, Desikan R, Hancock J. 2002. Hydrogen peroxide signaling. *Curr Opin Plant Biol*. 5(5):388–395. [https://doi.org/10.1016/S1369-5266\(02\)00282-0](https://doi.org/10.1016/S1369-5266(02)00282-0).
- Park SW, Li W, Viehhauser A, He B, Kim S, Nilsson AK, Andersson MX, Kittle JD, Ambavaram MM, Luan S, Esker AR, Tholl D, Cimini D, Ellerstrom M, Coaker G, Mitchell TK, Pereira A, Dietz KJ, Lawrence CB. 2013. Cyclophilin 20-3 relays a 12-oxo-phytyldienoic acid signal during stress-responsive regulation of cellular redox homeostasis. *Proc Natl Acad Sci USA*. 110(23):9559–9564. <https://doi.org/10.1073/pnas.1218872110>.
- Sakamoto W, Tamura T, Hanba-Tomita Y, Murata M. 2002. The *VARI* locus of *Arabidopsis* encodes a chloroplastic FtsH and is responsible for leaf variegation in the mutant alleles. *Genes Cells*. 7(8):769–780. <https://doi.org/10.1046/j.1365-2443.2002.00558.x>.
- Shi Y, Huang Y, Guo X, Lin X, Fang W. 2009. Comparison of chlorophyll fluorescence parameters in four cultivars of *Phyllostachys nigra*. *Acta Agric Univ Jiangxiensis*. 31(3):397–401. <https://doi.org/10.3969/j.issn.1000-2286.2009.03.004>.
- Sun Y, Hung C, Qiu J, Chen J, Kittur FS, Oldham CE, Henny RJ, Burkey KO, Fan L, Xie J. 2017. Accumulation of high OPDA level correlates with reduced ROS and elevated GSH benefiting white cell survival in variegated leaves. *Sci Rep-UK*. 7(1):44158. <https://doi.org/10.1038/srep44158>.
- Taiz L, Miller IM, Murphy A, Zeiger E. 2023. *Plant physiology and development* (7th ed). Oxford University Press, New York, NY, USA.
- Torrens-Spence MP, Bobokalonova A, Carballo V, Glinkerman CM, Pluskal T, Shen A, Weng JK. 2019. PBS3 and EPS1 complete salicylic acid biosynthesis from isochorismate in *Arabidopsis*. *Mol Plant*. 12(12):1577–1586. <https://doi.org/10.1016/j.molp.2019.11.005>.
- Ullah C, Chen YH, Ortega MA, Tsai CJ. 2023. The diversity of salicylic acid biosynthesis and defense signaling in plants: Knowledge gaps and future opportunities. *Curr Opin Plant Biol*. 72:102349. <https://doi.org/10.1016/j.pbi.2023.102349>.
- Wang A. 2016. The research on the application of ornamental bamboo in the landscape of Changsha City (MS Thesis). Central South University of Forestry and Technology, Changsha, Hunan, China. <https://doi.org/10.7666/d.Y3134582>.
- Wang H, Wang J. 2012. Effects of salicylic acid on plant antioxidant capacity under abiotic stress. *Bull Biol*. 47(2):16–18. <https://doi.org/10.3969/j.issn.0006-3193.2012.02.006>.
- Wasternack C, Hause B. 2018. A bypass in jasmonate biosynthesis—the OPR3-independent formation. *Trends Plant Sci*. 23(4):276–279. <https://doi.org/10.1016/j.tplants.2018.02.011>.
- Wu J, Zhu W, Zhao Q. 2023. Salicylic acid biosynthesis is not from phenylalanine in *Arabidopsis*. *J Integr Plant Biol*. 65(4):881–887. <https://doi.org/10.1111/jipb.13410>.
- Wu X, Guo X, Wang S, Wang D, Wu Z, Lü Z, Zhang Z, Du K. 2018. Effect of iron-supply to the half root on chlorophyll fluorescence parameters of *Pyrus betulaefolia* seedlings. *Guoshu Xuebao*. 35(S1):125–130. <https://doi.org/10.13925/j.cnki.gsx.2018.S.20>.
- Wu Z, Li W, Xiong D, Wang S, Zhou Y. 2013. Comparative study on photosynthetic and fluorescence characteristics among different aged *Bambusa textilis*. *Xibei Linxueyuan Xuebao*. 28(6):33–36. <https://doi.org/10.3969/j.issn.1001-7461.2013.06.06>.
- Yang Y, Zhang R, Leng P, Hu Z, Shen M. 2018. Effect of exogenous salicylic acid on the physiological and biochemical processes of *Ligustrum lucidum* during natural cold acclimation. *HortScience*. 53(6):859–864. <https://doi.org/10.21273/HORTSCI12949-18>.
- Yin J, Yang H, Peng L, Huang M, Tang Z, Li J, Li C. 2016. Preliminary research on the etiolation leaf-color mutant Bn.ell in *Brassica napus*. *J Southwest Univ*. 38(5):1–6. <https://doi.org/10.13718/j.cnki.xdsk.2016.05.001>.
- Yu F, Fu A, Aluru M, Park S, Xu Y, Liu H, Liu X, Foudree A, Nam-bogga M, Rodermel S. 2007. Variegation mutants and mechanisms of chloroplast biogenesis. *Plant Cell Environ*. 30(3):350–365. <https://doi.org/10.1111/j.1365-3040.2006.01630.x>.
- Yu S. 2018. Study on the differences of photosynthesis and peroxidation system in the green and white tissues of *Ananas comosus* var. *bracteatus* (MS Thesis). Sichuan Agricultural University, Chengdu, Sichuan, China.
- Zhu X, Zhang H, Nan W. 2017. Research progress on regulation of ABA in plant root development. *Chih Wu Sheng Li Hsueh T'ung Hsun*. 53(7):1123–1130. <https://doi.org/10.13592/j.cnki.ppj.2016.0500>.